

EFFECTS OF THE MEASURED NOISE ON THE FAILURE MECHANISM OF PRE-CRACKED CONCRETE SPECIMENS UNDER THE LOADING MODES I, II, III, AND IV

J. Fu,^a H. Haeri,^{a,1} M. D. Yavari,^b V. Sarfarazi,^c
and M. F. Marji^d

UDC 539.4

The diagrams for damage location and convergence curves based on the differential evolutionary algorithms under the loading modes I, II, III, and IV are studied for the pre-cracked concrete specimens with a center crack of different inclination angles and considering the noise effect. The numerical results for the modeled specimens showed that the measured noise may have significant effects on these diagrams, especially when the center cracks are of high inclination angles (greater than 45°) with respect to the applied loading direction. It was also shown that the measured noise might distort the accelerations in the damaged concrete specimens, which highlighted the effectiveness of the present algorithm provided via MATLAB. In this study, an algorithm is established in the MATLAB software to numerically simulate the noise effect on the damage location and convergence diagrams for the cubic concrete specimens based on the differential evolutionary algorithm. The particle flow code for two-dimensional (PFC2D) problems was used to simulate crack propagation paths in the numerically failed pre-cracked concrete specimens.

Keywords: measured noise, convergence diagram, damage location, MATLAB, cubic pre-cracked concrete specimen.

Introduction. The failure mechanism of concrete specimens under various loading conditions is important for the design and construction of concrete structures and studied by many investigators. On the other hand, identification and detection of the concrete damages need to consider the damage mechanism of these brittle materials by developing some sophisticated methods. There are two main categories for detecting the structural damages in the constructing materials, i.e., the destructive and nondestructive methods. The destructive methods mainly involve laboratory tests on materials' specimens until their failure. The nondestructive methods include the local and general detection methods. There are some limitations for the local damage detection methods, such as penetration depth of the waves and the defect location for performing the test [1]. Tiachacht et al. [2] investigated the effect of mode orders on the detectability of possible damages to structures. They used the continuous wavelet transform of normalized mode shapes to detect the possible damage location and intensity of cracks in beams. Their findings show that the higher is the order of investigated mode shape, the more reliable results are achieved, which shows the sensitivity of higher modes [2]. In another work, Janeliukstis et al. [3] proposed a method for detecting damage in structures using the finite element method (FEM), whose goal was to use the advantages of wavelet transform in detecting and locating small structural damages. In their proposed method, the mixed Gaussian

^aSchool of Civil Engineering and Transportation, North China University of Water Resources and Electric Power, Zhengzhou, China (haerihadi@gmail.com; h.haeri@bafgh-iau.ac.ir). ^bDepartment of Mining Engineering, Islamic Azad University, Bafgh Branch, Bafgh, Yazd, Iran. ^cDepartment of Mining Engineering, Hamedan University of Technology, Hamedan, Iran. ^dDepartment of Mine Exploitation Engineering, Faculty of Mining and Metallurgy, Institute of Engineering, Yazd University, Yazd, Iran. Translated from Problemy Prochnosti, No. 6, p. 118, November – December, 2021. Original article submitted January 19, 2021.

continuous wavelet transform was used to obtain the distribution of wavelet coefficients, in order to detect the location of defects in a square-shaped plate [4].

Kaewunruen et al. [5] presented a fast and effective method for finding the location and depth of crack through the changes in the natural frequency of the structure [5, 6]. Zhang et al. [7] took into account the nonlinear terms associated with crack intensity to propose a new method for the detection of an unknown number of cracks in the structures using the natural frequency calculation process [7]. In another study, Pimentel et al. [8] indicated how bending cracks alter the vibrating properties, such as frequency response function, and how to use these properties to identify the damage. In their study, the crack was modeled in the form of torsion spring, and vibrating properties such as the natural frequency and mode shape were investigated to identify the structural damage [8]. Ravanfar et al. [9] presented a two-phase method for determining the location and severity of damage flexural vibration. Moreover, the effect of mode order and the distance of damage from the base was also examined. It was revealed that the distance of cracks from each other have no effect on finding their locations [9]. There are mainly two general approaches for considering the mechanism of damage (i.e., the continuum damage theory) and fracture (i.e., the linear elastic fracture mechanics) in brittle materials such as concrete and rocks. Based on these two approaches, many experimental and numerical investigations were accomplished to study the fragmentation and damage of the geo-materials such as concrete and rocks [10–18]. In this study, the effect of noise on various diagrams indicating the damage location and predicting the convergence based on the differential evolutionary algorithm is considered for the pre-cracked cubic concrete specimens with a center crack of different inclination angles. These diagrams are provided by establishing the algorithm in MATLAB considering four modes (I, II, III, and IV) for the tested concrete specimens. The PFC2D software is also used in this study to numerically simulate the crack propagation paths of the single-crack cubic specimens and the damage location and the convergence diagram of the differential evolutionary algorithm.

1. Methodology. The crack propagation paths of the single-crack cubic specimens have been numerically investigated by a versatile discrete element code known as Particle Flow Code (PFC2D). The MATLAB software is used in this study to numerically simulate the damage location and the convergence diagram of the differential evolutionary algorithm.

This study attempted to investigate the breakage process and noise effect in pre-cracked cubic specimens containing a single crack in the central part with inclination angles of 45, 60, 35, and 75° to the loading direction. The damage location and the convergence diagram of differential evolutionary algorithm were obtained with consideration of a 3% measurement noise under four modes I (opening mode), mode II (shearing mode), mode III (tearing mode), mode IV (in-plane axial mode or in-plane buckling mode) in the pre-cracked cubic specimens of concrete. For each specimen, the parametric analysis and the optimization algorithm implied a 3% noise.

2. Numerical Model.

2.1. Particle Flow Code. The polygonal grain geometry of the particles in a particle assembly, as proposed by Potyondy [19], was used to simulate the real joints in the geo-material in the form of flat joint (FJ) models. As shown in Fig. 1, the particle contacts were represented by local flat notional surfaces, while faced grains were represented by circular (2D) or spherical (3D) shapes at the skirted face [19].

2.2. Preparation and Calibration of the PFC2D Model for Rock-Like Material. To simulate the concrete or other geo-material specimens with PFC2D, the Brazilian test (Fig. 2) is usually used to calibrate the software. Then, the calibrated microproperties given in Table 1 were used for the concrete specimens' modeling. Table 2 lists the well matched numerical and experimental results of the mechanical characteristics of concrete specimens.

2.3. Numerical Simulation of Specimens Containing the Inclusion. The modeled tests for uniaxial compression of the concrete specimens, as shown in Fig. 3a–3d, correspond to the notch's inclination angles of 45, 60, 35, and 75°, respectively. The particle assembly was modeled via the calibrated PFC2D using 12,456 circular discs with 0.27 radii for the modeled specimens (four different models) of 150 × 150 mm in size.

2.4. Failure Mechanism of the Numerical Model. The failure and fracture mechanisms of the modeled concrete specimens are shown in Fig. 4a–4d, respectively, considering central crack's inclination angles of 45, 60, 35, and 75°.

TABLE 1. Microfeatures Utilized to Characterize the Concrete

Particle microproperties		Flat-joint microproperties	
Model height (mm)	108	Gap ratio	0.5
Model width (mm)	54	E_c (GPa)	5
Stiffness ratio (kN/s)	2	Bonded friction	0.9
Density (g/cm^3)	3000	Tensile strength (MPa)	0.3
Minimum particle diameter	0.54	Standard deviation of tensile strength (MPa)	0.03
Maximum particle diameter	1.08	Cohesion (MPa)	0.9
E_c (GPa)	5	Cohesion standard deviation (MPa)	0.09
Porosity	0.08	Number of elements	2

TABLE 2. Tensile Properties Used in the Numerical Models

Experimental results		Numerical outputs	
Tensile strength of concrete (MPa)	2.45	Tensile strength of concrete (MPa)	2.40

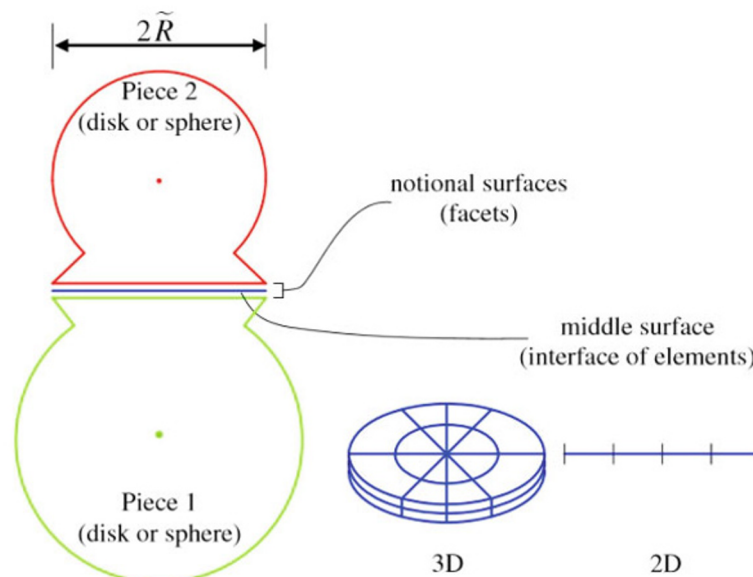


Fig. 1. The flat joint model [16].

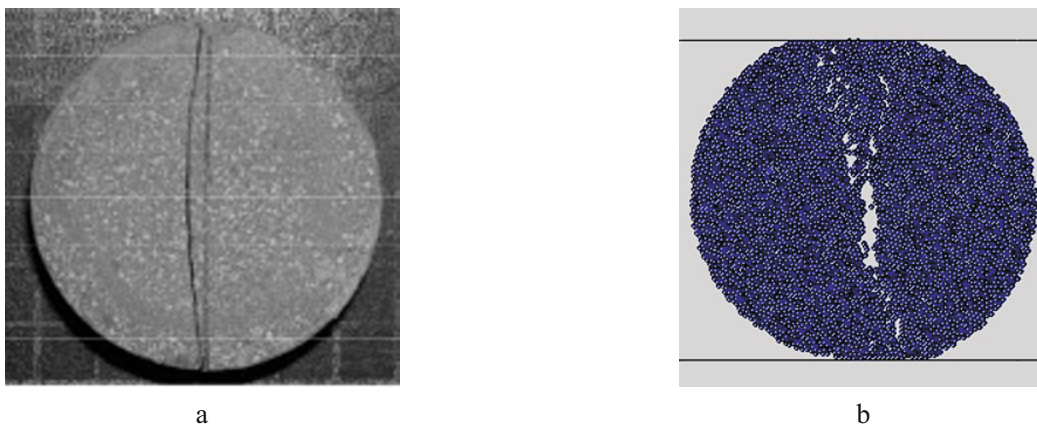


Fig. 2. Brazilian test of concrete: specimen (a) and its numerical simulation (b).

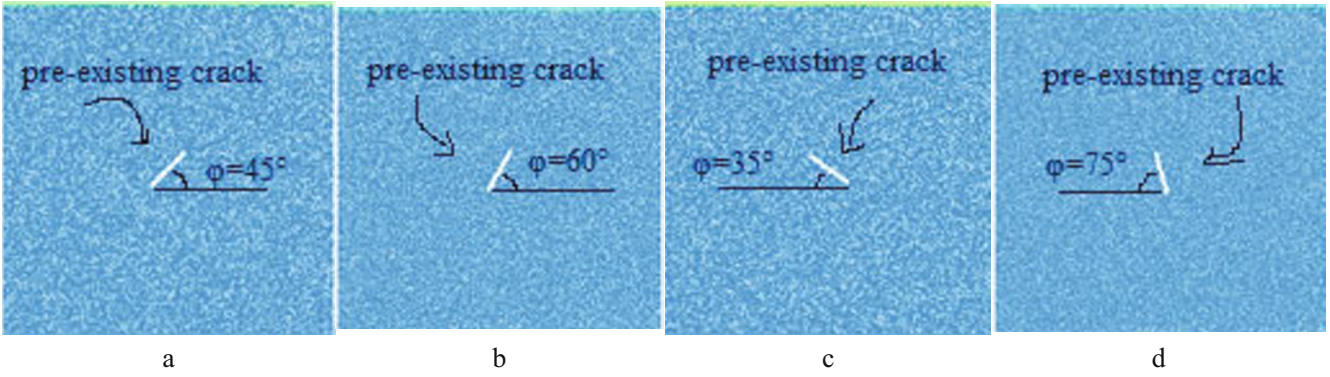


Fig. 3. Models containing one notch with inclination angles: (a) $\phi = 45^\circ$, (b) $\phi = 60^\circ$, (c) $\phi = 35^\circ$, and (d) $\phi = 75^\circ$.

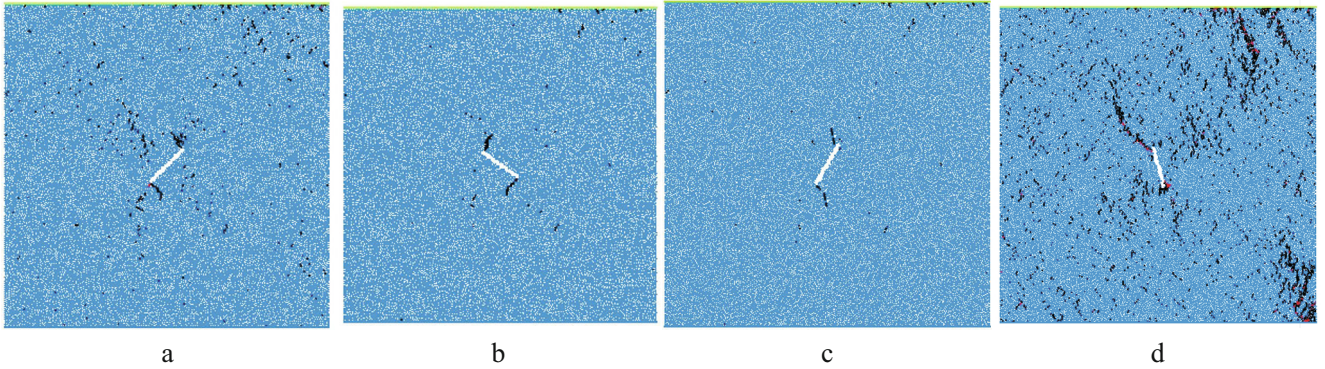


Fig. 4. Failure patterns of models containing a notch with inclination angle: (a) 45° , (b) 60° , (c) 35° , and (d) 75° .

3. Investigating the Results with the Measurement Noise. The effect of the measured noise on the effectiveness of the proposed damage detection algorithm is discussed in this section. This effect was presented by considering a $\pm 3\%$ standard error due to the measured noise. The effect of this noise on the measured accelerations of the damaged concrete specimen was assessed as follows:

$$R \text{ Acceleration } D = \text{Acceleration } D \times [1 + (2(\text{random}) - 1) \times \text{noise}], \quad (1)$$

where *noise* is the measured noise (preset at 3%), *random* is the function of the yielding positive values smaller than one, and designed by MATLAB software with the same size of the node acceleration vector of the damaged concrete specimen, *Acceleration D* and *R Acceleration D* are the vectors of node accelerations of the damaged concrete specimen without and with the measured noise effect, respectively.

In the following section, the obtained results are presented considering the measured noise effect.

3.1. Centered Single-Cracked Cubic Specimen with Crack Inclination Angle of 45° . In this section, the effect of noise on the damage mechanism of the centered single-cracked cubic specimen with a crack inclination angle of 45° is studied. The noise distorts the accelerations of the damaged concrete specimen. In this case, the effectiveness of the algorithm is even more highlighted.

Figure 5 depicts the damage identification diagrams in the presence of the measured noise. These diagrams show that the defined damage is approximately the same as that of the calculated one, which confirms the accuracy of the proposed method in detecting the damaged elements. These figures depict the diagrams for the concrete specimens containing a centered crack with a 45° inclination angle.

Figure 6 depicts the convergence diagrams of the optimization algorithm for the pre-cracked concrete specimens under modes I, II, and III. These figures show that after 400 iterations, the algorithm did not change significantly during the last 100 iterations and reached the desired convergence.

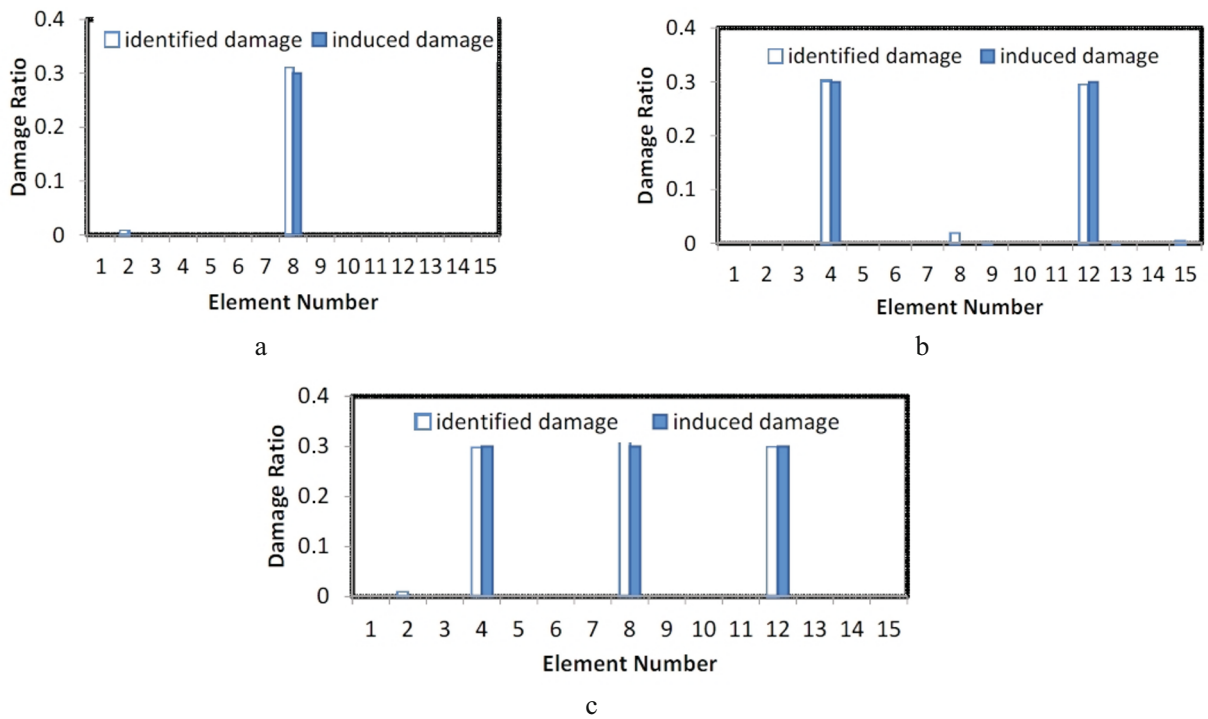


Fig. 5. Predicted damage locations in a centered single-cracked cubic specimen with crack's inclination angle of 45° with consideration of a 3% measurement noise under mode I (a), mode II (b), and mode III (c).

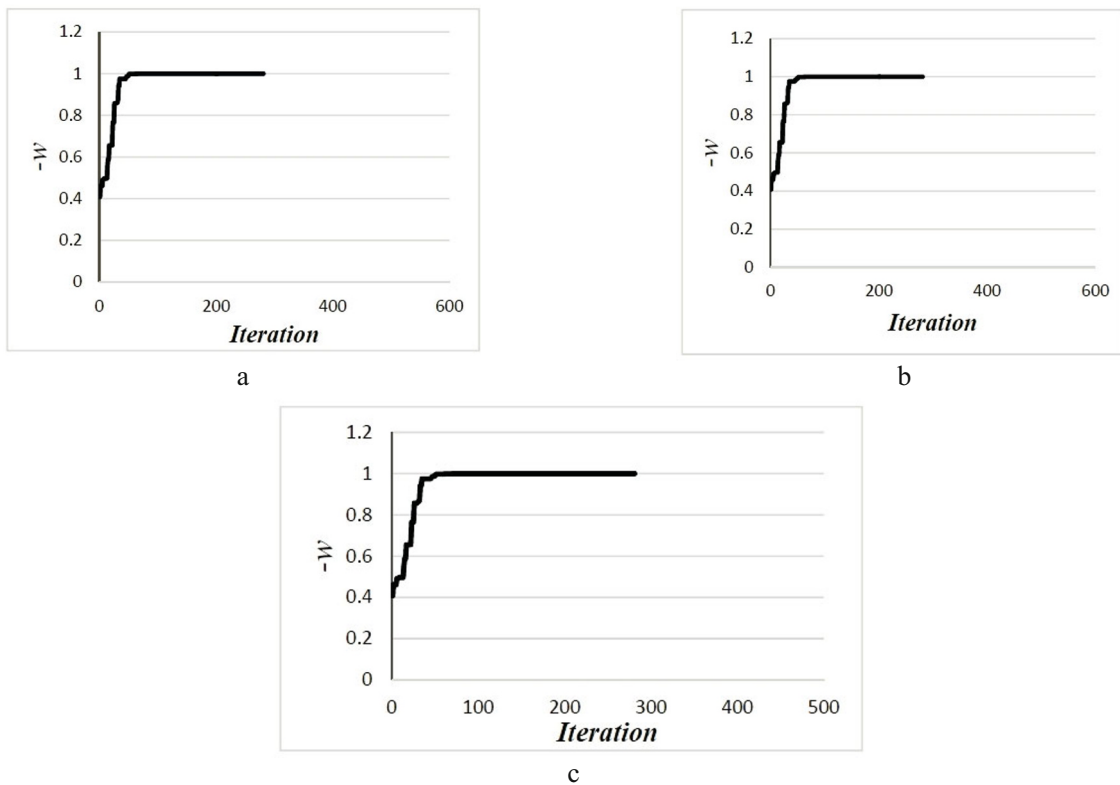


Fig. 6. Convergence of the differential evolutionary algorithm in a centered single-cracked cubic specimen with crack's inclination angle of 45° under modes I, II, and III considering a 3% of measured noise: diagram of the evolutionary algorithm for mode I (a), mode II (b), and mode III (c).

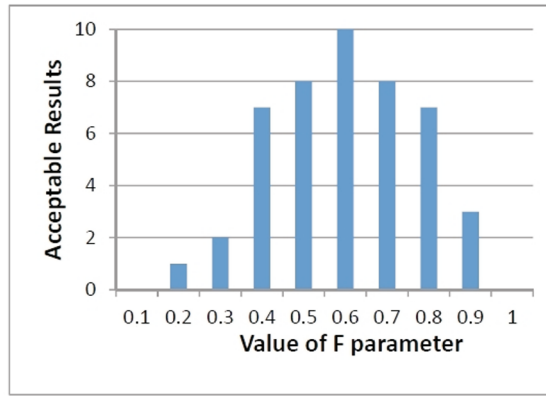


Fig. 7. Analysis of the parameter F used for the convergence of a centered single-cracked cubic specimen with a crack inclination angle of 45° under mode III.

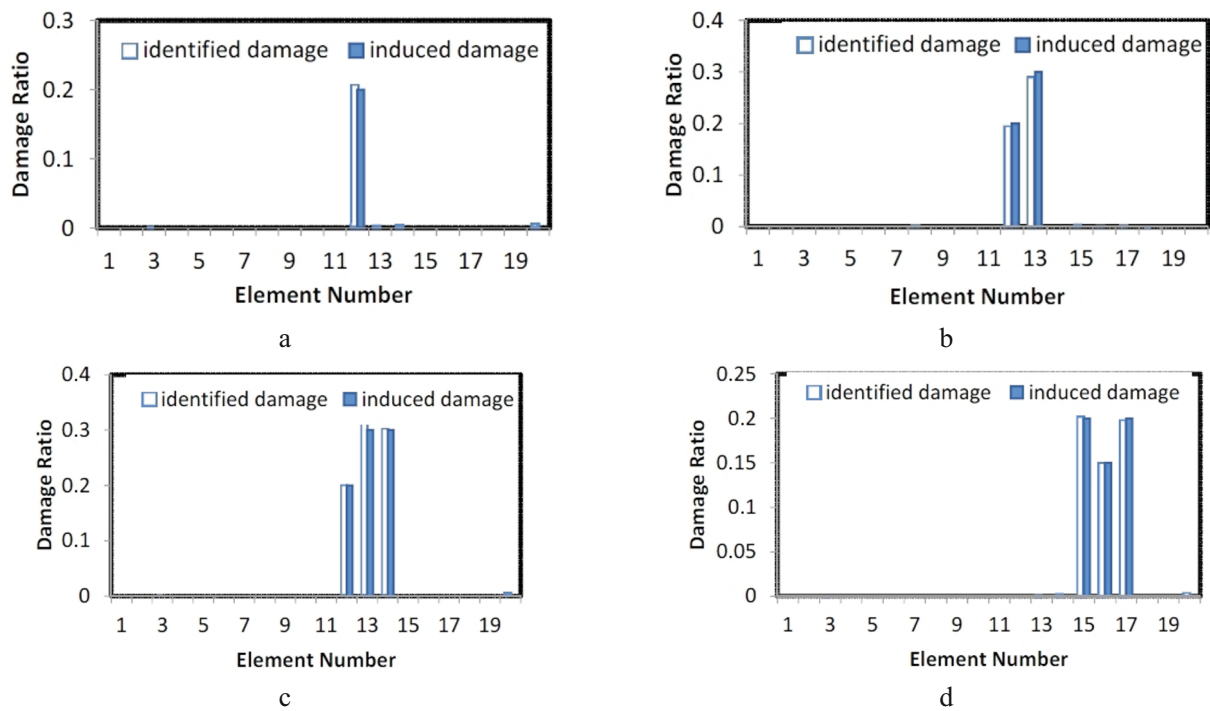


Fig. 8. Predicted damage locations in a centered single-cracked cubic specimen with a crack inclination angle of 60° , considering a 3% measurement noise under mode I (a), mode II (b), mode III (c), and mode IV (d).

3.2. Investigating the Parameter F in a Centered Single-Cracked Cubic Specimen with a Crack Inclination Angle of 45° under Mode III. The differential evolutionary diagrams, like other optimization diagrams, consist of certain parameters controlling the optimization process. One of these parameters is F , which is a function of the generating and mutant vectors. Since the differential evolutionary algorithm has not been used in the damage detection process for the concrete specimens, the trial-and-error method had to be used to obtain each parameter. For the F range from 0 to 1, the results plotted in Fig. 7 indicate that F parameter had its best performance at 0.6. The algorithm was repeated 10 times for each value and converged to its desired value when F reached 0.6. The number of iterations corresponding to the algorithm response for various values is shown in Fig. 7. It is noteworthy that the value of F was obtained via a trial-and-error method and can be used in the damage detection problems. In other cases, the best performance may be attained at different values of F .

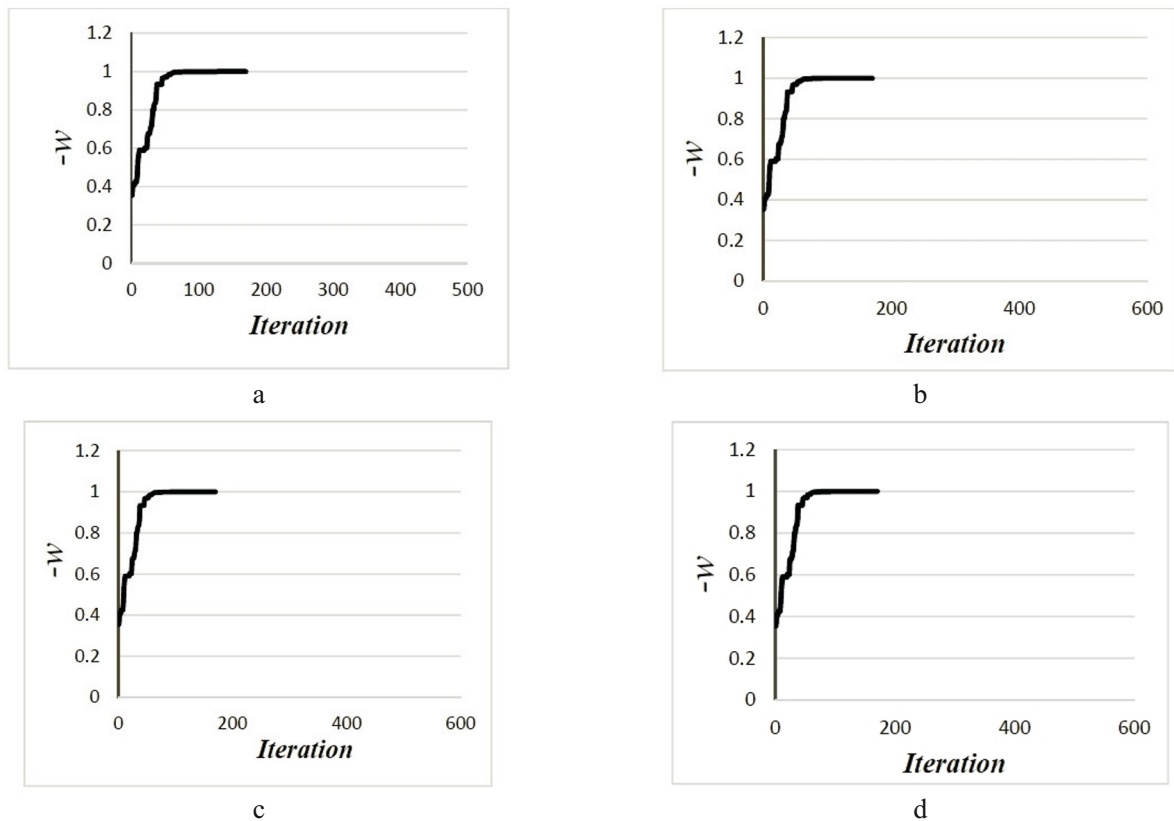


Fig. 9. Convergence of the differential evolutionary algorithm under the loading modes I (a), II (b), III (c), and IV (d) for a centered single-cracked concrete specimen with a crack inclination angle of 60° and considering a measured noise of 3%.

3.3. The Centered Single-Cracked Cubic Specimen with a Crack Inclination Angle of 60° . In this section, the noise effect on the damage mechanism of the centered single-cracked cubic specimen with a crack inclination angle of 60° is considered. The noise may distort the accelerations of the damaged concrete specimen so that the effectiveness of the algorithm is even more highlighted. The noise effect was preset at $\pm 3\%$ and obtained according to Eq. (1). Figure 8 depicts the damage identification diagrams due to the noise effect for the concrete specimens under the modes I, II, III, and IV. These diagrams show that the defined damage is approximately the same as that of the real one, which confirms the accuracy of the proposed method for detecting the damaged elements. Figure 9 shows the damage identification for a concrete specimen containing a center crack with a crack inclination angle of 60° . The optimization algorithm converges under the loading modes I, II, III, and IV for this specimen.

As shown in Fig. 9, after 300 iterations, the algorithm did not change significantly in the last 100 iterations and converged to the desired value of the parameter.

3.4. Examining parameter CR in the Centered Single-Cracked Cubic Specimen with a Crack Inclination Angle of 60° under Mode IV. The differential evolutionary diagram, like the other optimization diagrams, consists of certain parameters controlling the optimization process. One of these parameters is the CR parameter. Since the differential evolutionary algorithm has not been used in the damage detection of concrete specimens yet, the trial-and-error method was used to obtain each proper parameter. As the value of CR ranged between 0 and 1, the analysis of this parameter was performed, as shown in Fig. 10. The parameter had the best performance at $CR = 0.3$. The algorithm was repeated 10 times for each value, being systematically converged at $CR = 0.3$. The number of iterations for the algorithm to make responses for various values of the parameters is shown in Fig. 10.

3.5. The Centered Single-Cracked Cubic Specimen with a 35° Crack Inclination Angle. In this section, the effect of noise was considered in the failure analysis of the cubic concrete specimen with a center crack inclined at

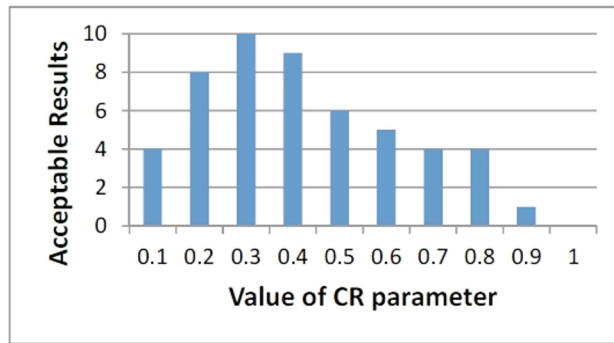


Fig. 10. Convergence in the *CR* parameter for a centered single-cracked cubic specimen with a crack inclination angle of 35° .

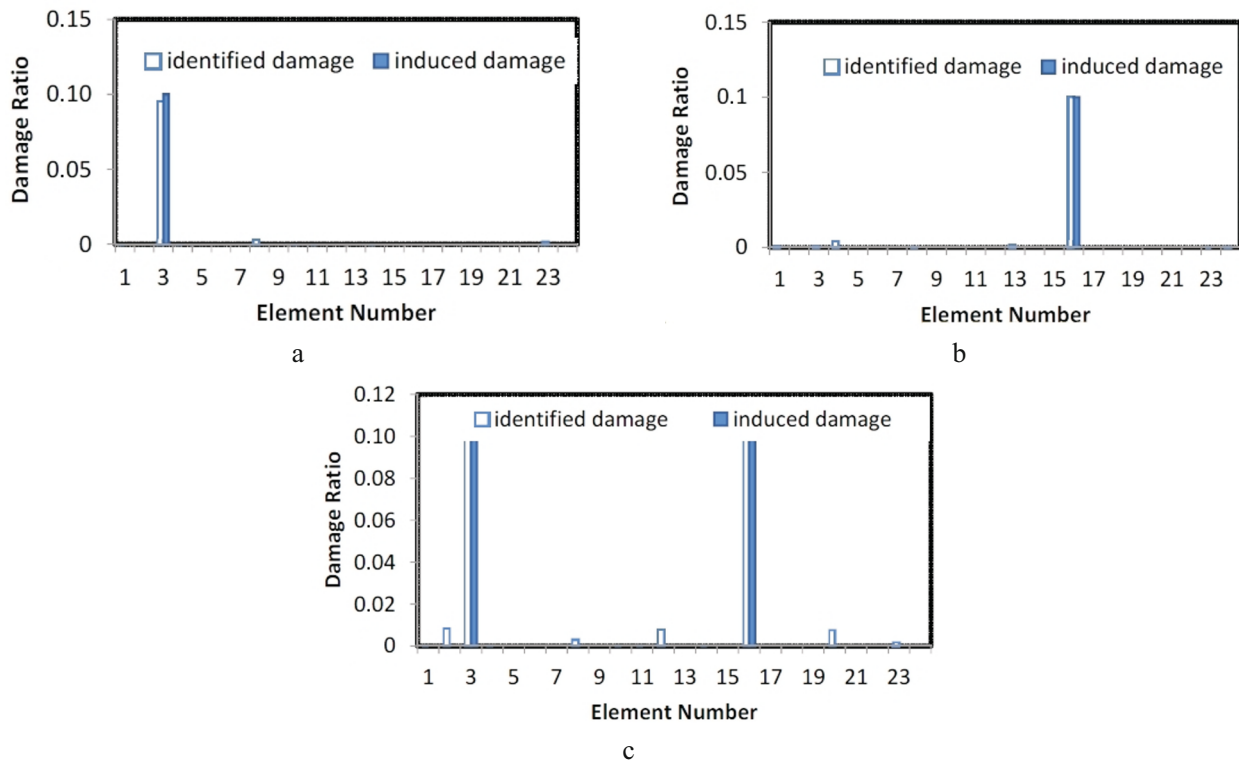


Fig. 11. Predicted damage locations in cubic concrete specimens with a single center crack with a 35° inclination angle under modes I (a), II (b), and III (c), with a 3% measured noise effect.

35° to the loading axis. The noise effect distorted the accelerations of the damaged concrete specimen so that the effectiveness of the algorithm was even more highlighted. The other influencing parameters were the same as those previously mentioned in this research. The noise effect in this failure analysis was $\pm 3\%$, which was obtained according to Eq. (1). Figure 11 depicts the damage identification diagrams considering the noise effect for the specimens under modes I, II, and III. These diagrams show that the defined damage was approximately the same as that of the measured damage, confirming the high accuracy of the proposed method in detecting the damaged elements in the concrete specimens.

The damage identification diagram and the optimization algorithm convergence diagram for a centered single-cracked cubic specimen with a crack inclination angle of 35° and modes I, II, and III are shown in Fig. 12.

As seen in Fig. 12, after 800 iterations, the algorithm reached convergence at the last 500 iterations, with no significant changes observed in the results.

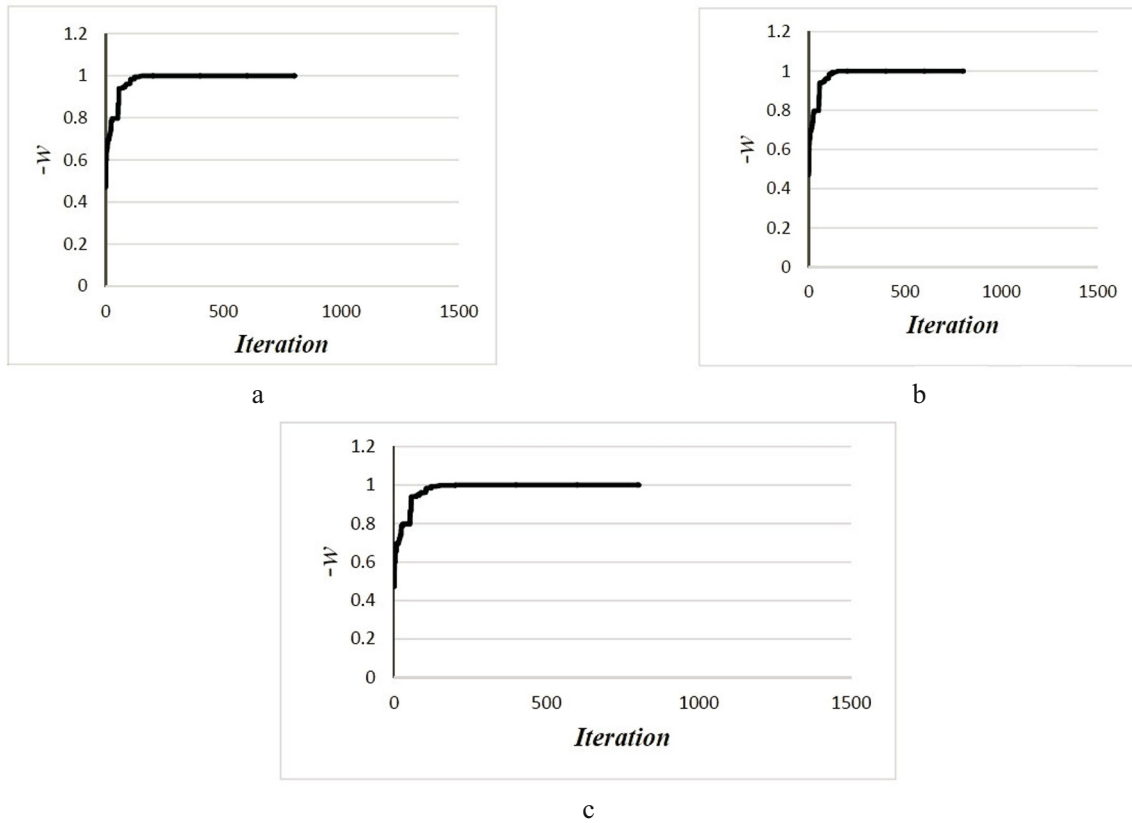


Fig. 12. Convergence of the differential evolutionary algorithm for modes I (a), II (b), and III (c) in a centered single-cracked cubic specimen with crack inclination angle of 35° considering a 3% measured noise effect.

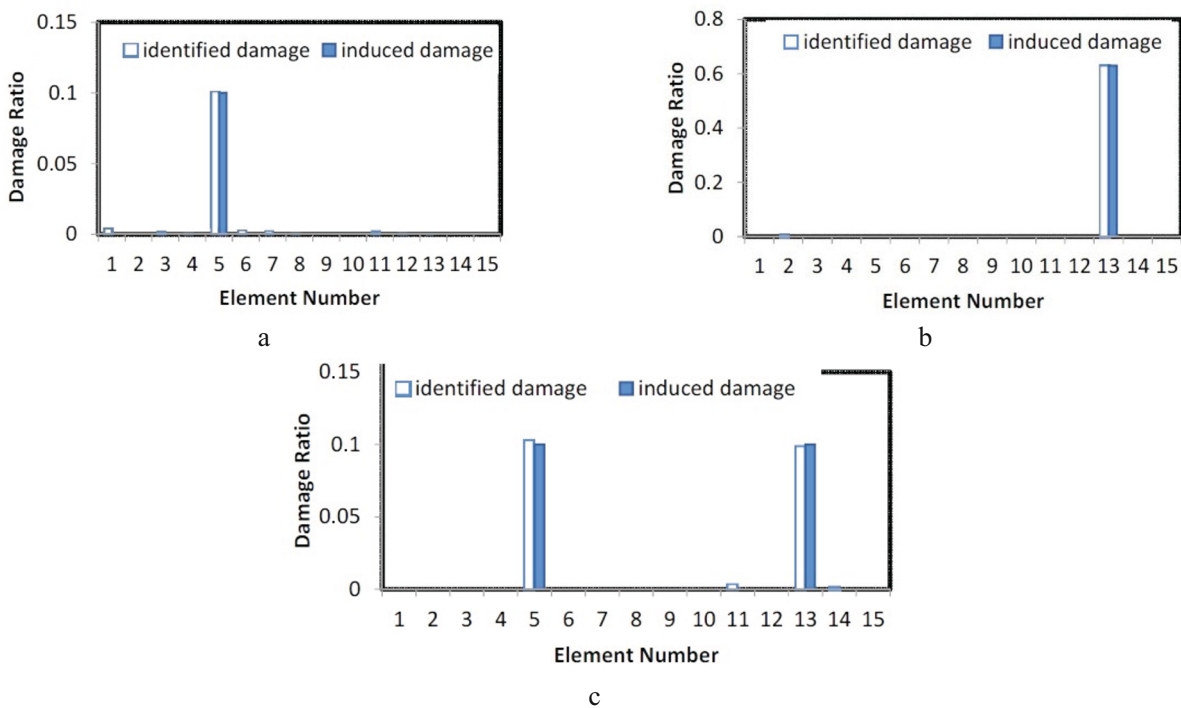


Fig. 13. Predicted damage locations for modes I (a), II (b), and III (c) of loading conditions in a single-cracked cubic specimen with a center crack inclined at 75° considering a 3% measured noise effect.

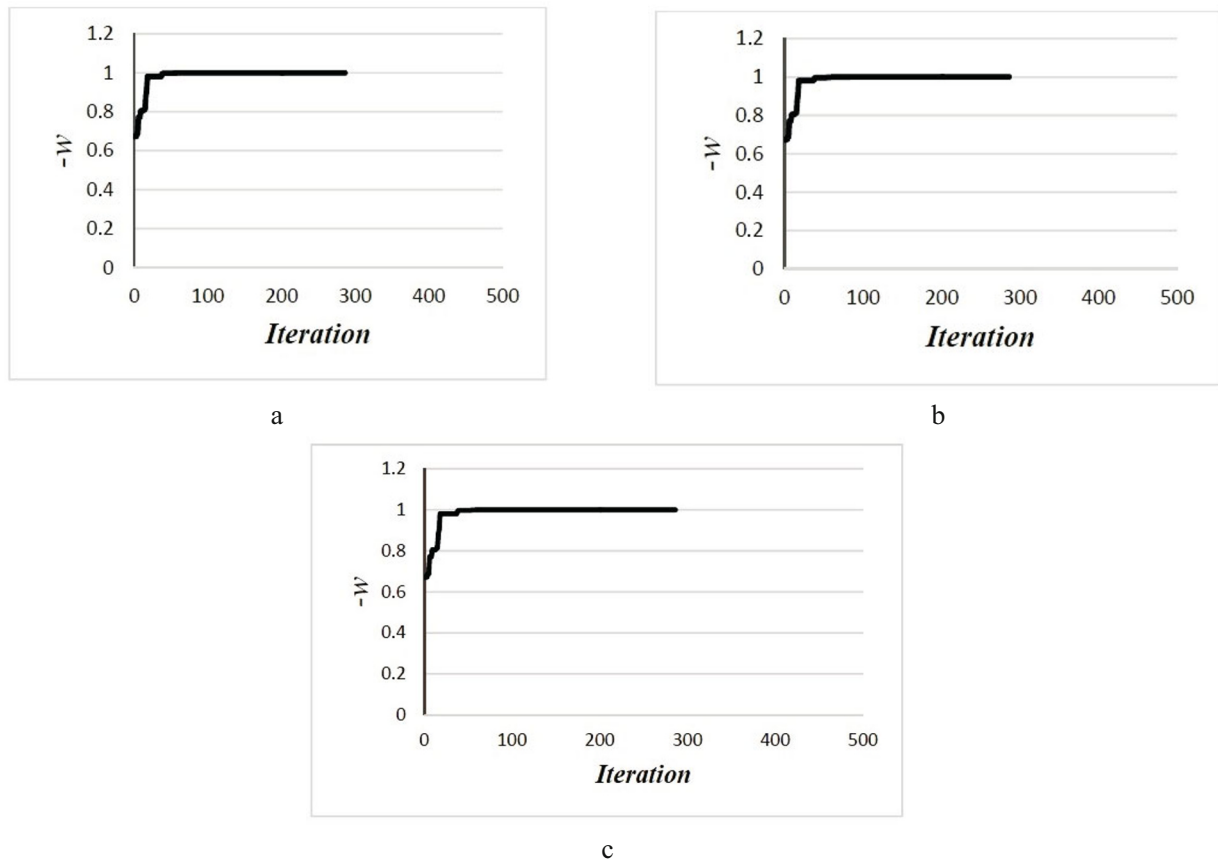


Fig. 14. Convergence of differential evolutionary algorithm under modes I (a), II (b), and III (c) in a centered single-cracked cubic specimen with a crack inclination angle of 75° and a 3% measurement noise.

3.6. The Centered Single-Cracked Cubic Specimen with Crack Inclination Angle of 75° . The noise effect on the failure process of the cubic concrete specimens containing a centered single-crack with a 75° inclination angle is considered in this section. All other parameters were the same as in the previous cases. The noise effect was preset at $\pm 3\%$ via Eq. (1). Figure 13 presents damage identification diagrams with a 3% noise for modes I, II, and III. These diagrams show that the defined damage was approximately the same as that obtained for real damage, which confirms the accuracy of the proposed method in detecting the damaged elements in the concrete specimens.

The damage identification diagrams and the optimization algorithm convergence diagrams in the concrete specimen with a center crack of 75° inclination to the loading axis for modes I, II, and III are shown in Fig. 14.

As seen in these diagrams, after 300 iterations, the algorithm reached convergence during the last 100 iterations, showing the effectiveness and correctness of the present analysis.

Conclusions. In this study, the damage locations and convergence diagrams of the differential evolutionary algorithm under modes I, II, III, and IV in cubic concrete specimens containing a single center crack with different inclination angles were investigated, taking into account the measured noise effect.

The crack propagation paths in the single-crack cubic specimens were numerically simulated by a versatile discrete element code referred to as Particle Flow Code (PFC2D). The MATLAB software was used in this study to numerically simulate the damage locations and plot convergence diagrams of the differential evolutionary algorithm.

The parametric analysis and optimization algorithm were realized considering a 3% noise effect. To calculate the accelerations, Newmark's method was used. At first, the damage detection problem was reduced to an optimization problem. The noise effects were considered, and the optimization problem was solved using the

differential evolutionary algorithm. To examine the effectiveness of the proposed method and the damage detection process, the modeling was carried out with reduced elastic moduli of the elements. It was concluded that the measured noise might have significantly bias these diagrams, especially, in the case of central cracks with high inclination angles (over 45°) to the applied loading direction.

REFERENCES

1. T. Vo-Duy, V. Ho-Huu, H. Dang-Trung, et al., “Damage detection in laminated composite plates using modal strain energy and improved differential evolution algorithm,” *Procedia Engineer.*, **142**, 182–189 (2016).
2. S. Tiachacht, A. Bouazzouni, S. Khatir, et al., “Damage assessment in structures using combination of a modified Cornwell indicator and genetic algorithm,” *Eng. Struct.*, **177**, 421–430 (2018).
3. R. Janeliukstis, S. Rucevskis, M. Wesolowski, et al., “Damage identification in beam structure using spatial continuous wavelet transform,” *IOP Conf. Ser.-Mat. Sci.*, **96**, No. 1, 012058 (2015), <https://doi.org/10.1088/1757-899X/96/1/012058>.
4. M. A. Livani, N. Khaji, and P. Zakian, “Identification of multiple flaws in 2D structures using dynamic extended spectral finite element method with a universally enhanced meta-heuristic optimizer,” *Struct. Multidiscip. O.*, **57**, No. 2, 605–623 (2018).
5. S. Kaewunruen, A. Aikawa, and A. M. Remennikov, “The importance of ‘dynamics’ in the design and performance-based testing criteria for railway track components,” *Procedia Struct. Integr.*, **21**, 83–90 (2019).
6. M. Jahjouh and R. Rolfes, “The performance of a modified harmony search algorithm in the structural identification and damage detection of a scaled offshore wind turbine laboratory model,” in: H. C. Rodrigues et al. (Eds.), *EngOpt 2018 Proceedings of the 6th International Conference on Engineering Optimization*, Springer (2019), pp. 185–199.
7. X. Zhang, R. Chen, and Q. Zhou, “Damage identification using wavelet packet transform and neural network ensembles,” *Int. J. Struct. Stab. Dyn.*, **18**, No. 12, 1850148 (2018), <https://doi.org/10.1142/S0219455418501481>.
8. R. Pimentel, T. Guedes, L. Melo, et al., “Damage detection assessment in reinforced concrete slabs using impact tests,” *Procedia Engineer.*, **199**, 1976–1981 (2017).
9. S. A. Ravanfar, H. A. Razak, Z. Ismail, and H. Monajemi, “An improved method of parameter identification and damage detection in beam structures under flexural vibration using wavelet multi-resolution analysis,” *Sensors (Basel)*, **15**, No. 9, 22750–22775 (2015), <https://doi.org/10.3390/s150922750>.
10. M. F. Marji, H. Hosseini-Nasab, and A. H. Kohsary, “A new cubic element formulation of the displacement discontinuity method using three special crack tip elements for crack analysis,” *JP J. Solids Struct.*, **1**, No. 1, 61–91 (2007).
11. Y. Xia, B. Chen, S. Weng, et al., “Temperature effect on vibration properties of civil structures: a literature review and case studies,” *J. Civil Struct. Health Monit.*, **2**, 29–46 (2012), <https://doi.org/10.1007/s13349-011-0015-7>.
12. W. Xu, M. Cao, W. Ostachowicz, et al., “Two-dimensional curvature modeshape method based on wavelets and Teager energy for damage detection in plates,” *J. Sound Vib.*, **347**, 266–278 (2015).
13. H. Haeri and M. F. Marji, “Simulating the crack propagation and cracks coalescence underneath TBM disc cutters,” *Arab. J. Geosci.*, **9**, No. 2, 124 (2016), <https://doi.org/10.1007/s12517-015-2137-4>.
14. V. Sarfarazi, H. Haeri, M. F. Marji, and Z. Zhu, “Fracture mechanism of Brazilian discs with multiple parallel notches using PFC2D,” *Period. Polytech.-Civ.*, **61**, No. 4, 653–663 (2017).
15. R. Ghiasi, M. R. Ghasemi, and M. Noori, “Comparative studies of metamodeling and AI-Based techniques in damage detection of structures,” *Adv. Eng. Softw.*, **125**, 101–112 (2018).
16. S. R. H. Vaez and N. Fallah, “Damage identification of a 2D frame structure using two-stage approach,” *J. Mech. Sci. Technol.*, **32**, No. 3, 1125–1133 (2018).

17. M. Gordan, H. A. Razak, Z. Ismail, and K. Ghaedi, "Data mining based damage identification using imperialist competitive algorithm and artificial neural network," *Lat. Am. J. Solids Stru.*, **15**, No. 8 (2018), <https://doi.org/10.1590/1679-78254546>.
18. V. Jayalakshmi, K. Lakshmi, and A. Rama Mohan Rao, "Reconstruction of impact load on structures with limited measurements using dynamic hybrid adaptive differential search algorithm," *Inverse Probl. Sci. En.*, **28**, No. 3, 340–373 (2019).
19. D. O. Potyondy, "Simulating perforation damage with a flat-jointed bonded-particle material," Paper presented at the 51st US Rock Mechanics/Geomechanics Symposium (San Francisco, California, USA), Paper Number: ARMA-2017-0223 (2017).